

Understanding the structure and the dynamics of magnetic fluids: coupling of experiment and simulation

G Mériguet¹, E Dubois¹, M Jardat¹, A Bourdon¹, G Demouchy¹,
V Dupuis¹, B Farago², R Perzynski¹ and P Turq¹

¹ Université P et M Curie—Paris 6, UMR-UPMC-CNRS-ESPCI 7612, Laboratoire LI2C,
Case 51, 4 place Jussieu, Paris F-75005, France

² Institut Laue Langevin, BP 156, 38042 Grenoble Cedex 9, France

E-mail: meriguat@ccr.jussieu.fr

Received 3 May 2006, in final form 13 July 2006

Published 8 September 2006

Online at stacks.iop.org/JPhysCM/18/S2685

Abstract

Experiments and Brownian dynamics simulations have been coupled in order to better understand structural and dynamical properties of ferrofluids, especially the role of the magnetic dipolar interaction. The ferrofluid used is a ‘home-made’ well defined suspension, the experimental characteristics of which are introduced in the modelled system. In this system, the determination of the structure using simulations and small angle neutron scattering (SANS) experiments shows no sign of chaining in the suspensions, both without and with a magnetic field. Nevertheless, on the scale of the interparticle distance, the structure is strongly anisotropic. This is at contrast with the weak anisotropy of the translational diffusion coefficient under magnetic field on the same scale. Moreover, on the macroscopic scale, both structure and translational dynamics are strongly anisotropic. Also the rotational diffusion is strongly modified if determined without field or after a weak orientation of the particles with a weak field. These results all emphasize the role of the collective phenomena associated with the dipolar interaction.

(Some figures in this article are in colour only in the electronic version)

1. Introduction

Magnetic fluids, or ferrofluids, are colloidal dispersions of magnetic nanoparticles in a liquid [1], the properties of which, for example viscosity, microstructure or apparent density, can be tuned in a constant magnetic field or in a field gradient. Therefore, numerous applications based on the magnetic dipolar interactions have been or can be developed [2, 3]. The understanding of the specific properties of ferrofluids compared to those of classical colloids is therefore an important question, which has attracted considerable interest in the literature. However, up to now, there is no clear and definitive answer on several points, in

particular the possible control of the formation of chains, of aggregates, of the structure under field or of the dynamical properties (see the review articles [4, 5] and references therein). The question we want to address here is therefore the role of the magnetic dipolar interaction in the structural and dynamic properties of these magnetic fluids. To tackle this question, we choose to couple experimental measurements with modelling by using Brownian dynamics. Numerical simulations allow (i) calculating average as well as local properties at several timescales and length scales and (ii) investigating the influence of one parameter independently of the others in order to better understand the experimental results. This coupled approach raises however several difficulties. Firstly, it is necessary to simplify the real experimental system, keeping only the most relevant parameters. Then, the values of these parameters have to be properly estimated in order to simulate a system close to the real one. Finally, measurable quantities have to be calculated and confronted with experiments. Such an approach which couples experiments and simulations is original, compared with the studies found in the literature, either based on experiments or on simulations, however usually not connected [4, 5]. Moreover, the aim here is an attempt at convergence of the experimental system and of the modelled system, as well as of the quantities determined in both cases. Indeed, in the present work, the studied magnetic fluid is a ‘home-made’ dispersion, electrostatically stabilized, which allows control of the composition, thus the features of the dispersions. In particular, the anisotropic dipolar contribution to the interparticle potential and its weight in the total potential can be adjusted. In the modelling, these dispersions are considered as a collection of monodisperse nanoparticles dispersed in a continuum, subjected to thermal energy, with averaged interparticle interactions. The parameters introduced in the simulations are then chosen using direct or indirect experimental determinations.

In the following, the experimental and simulated systems are first presented in detail. Then section 3 describes the influence of a constant uniform magnetic field on the structure of the suspensions. The dynamics is presented in section 4, beginning with the rotational dynamics, followed by the translational one, the latter without and with an applied magnetic field.

2. Systems

2.1. Experimental system

The experimental system that we shall discuss here is an aqueous ferrofluid constituted of maghemite γ - Fe_2O_3 nanoparticles synthesized by condensation of ionic iron in an alkaline solution [2, 6]. Magnetite Fe_3O_4 is obtained, which is then oxidized in maghemite in order to have a chemically stable material. The surface of the nanoparticles is coated with citrate molecules, which ensure a negative charge at neutral pH, compensated by sodium counterions. The structural charge is around $2e^- \text{ nm}^{-2}$ if the citrate concentration is higher than 0.002 mol l^{-1} [7]. The size polydispersity of the particles, which is described by a lognormal law (mean diameter d_0 , polydispersity σ), is reduced using a process of fractionation [8]. In order to increase the influence of the magnetic dipolar interaction while keeping colloidal stability, only the largest particles have been extracted from the original dispersion. In order to have enough material to carry out all the experiments on the same sample, few fractionation steps are performed, reducing the polydispersity from 0.35 down to 0.25. The measurement of the magnetization M versus the magnetic field H allows determination, from the initial susceptibility χ_0 of dilute ferrofluids at $H = 0$, of the ratio γ of the dipolar interaction to the thermal energy $k_{\text{B}}T$:

$$\gamma = \frac{\mu_0 \mu^2}{k_{\text{B}} T \bar{r}^3} = 3\chi_0 \quad (1)$$

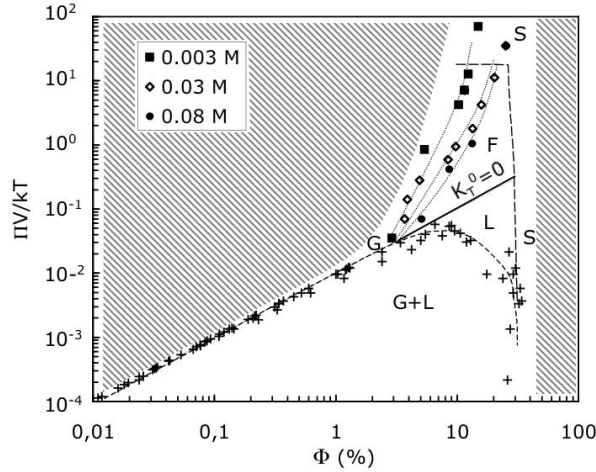


Figure 1. Phase diagram of aqueous ferrofluids based on γ - Fe_2O_3 , from previous works [12]. G, gas; L, liquid; F, fluid; S, solid. The hatched regions cannot be reached: packing limit at high ϕ , impossibility to increase the repulsion at low ϕ . The crosses are experimental data on the coexistence line between the gas and the liquid. The dashed lines are guides for the eye for the coexistence line between the gas and the liquid, and the limit between fluids and solids. The full straight line corresponds to a second virial coefficient K_0^T equal to zero. The data for the nanoparticles studied here are plotted in the graph for three sodium citrate concentrations (see legend).

where $\mu_0 = 4\pi \times 10^{-7} \text{ NA}^{-2}$, μ is the dipole moment, and \bar{r} is the mean interparticle distance. The determination of the volume fraction ϕ , thanks to a chemical titration of iron, yields the ratio γ/ϕ , specific to the nanoparticles [9, 10]. For dilute ferrofluids, where magnetic dipolar interactions are negligible, the adjustment of the magnetization curve to a Langevin's function weighted by a lognormal size distribution allows determination of a size distribution [2]. The parameters obtained for the ferrofluid studied here are $\gamma/\phi = 34$, $d_0 = 9.8 \text{ nm}$, $\sigma = 0.25$, with a magnetization of the material of $3.1 \times 10^5 \text{ A m}^{-1}$. The dispersions are then prepared by osmotic compression [11] using a polymer (dextran $110\,000 \text{ g mol}^{-1}$, Fluka) to impose the osmotic pressure Π . The ionic strength I is controlled by the sodium citrate concentration. With this process, Π , ϕ and I are known, which allowed us to determine the phase diagram of such systems in previous studies [12]: gas, liquid, fluid and solid phases can be obtained, as in an atomic system, depending on the location of the dispersion in the Π/ϕ phase diagram (see figure 1). In the present study, the samples considered are all located in the fluid area, thus the interparticle potential is globally repulsive, the repulsion range being tuned by the concentration of sodium citrate in the solution (see our three series of samples in figure 1), while the repulsion strength is controlled by the charge of the nanoparticles.

2.2. Modelling

In the modelled system, the nanoparticles are monodisperse with a diameter of 13 nm in order to recover the same dipolar interaction as in the real system ($\gamma/\phi = 34$). The magnetization of the material is the experimental value $3.1 \times 10^5 \text{ A m}^{-1}$. The dipole moment is linked to the axis of the nanocrystal, which corresponds to a rigid dipole [2]. The interparticle interaction has a dipolar anisotropic part and an isotropic part [13], the latter being modelled by a Yukawa

potential:

$$U_{\text{iso}}(r) = \frac{U_0}{\kappa r} e^{-\kappa(r-d)} \quad (2)$$

where $U_0/\kappa d$ is the interaction at contact and $1/\kappa$ is a characteristic screening length always larger than the ideal Debye length. Parameters U_0 and κ are estimated from a numerical adjustment of the structure factor of a concentrated dispersion ($\phi = 10\%$), measured using small angle neutron scattering (SANS) at $T = 298$ K [13]. Here $U_0 = 120$ kT and $\kappa^{-1} = 1.4$ nm. Moreover, at this mesoscopic scale, the coupling of the displacements of the particles mediated by the solvent, the so-called hydrodynamic interactions, have to be taken into account. However, they have no influence on the static properties. Here, they are calculated from the truncated expressions of the translational and rotational pair mobility tensors with stick boundary conditions, given in [14, 15]. The Brownian algorithm of Jones and Alavi [16] is used to compute the successive positions and orientations of all interacting nanoparticles. The cubic simulation box with periodic boundary conditions contains 500 or 1000 particles, in a medium reproducing water at 298 K. An Ewald summation allows us to evaluate the long ranged dipolar interactions. Simulations are performed with and without an external magnetic field. As they dramatically increase the computation time, hydrodynamic interactions are taken into account only if dynamical properties are computed. In addition, the use of the pairwise approximation is only valid up to volume fractions around 7%. Further simulation details may be found in [13, 17].

3. Modification of the structure in a magnetic field

If a magnetic field is applied, several phenomena can occur. Firstly, the particles tend to orientate along the field, secondly, the microscopic structure can be modified, and thirdly, a phase separation into a gas and a liquid phase can be induced. All these changes can be experimentally quantified by magnetization measurements, birefringence measurements (the nanoparticles being optically anisotropic [18]), small angle scattering or optical microscopy. Numerical simulations with an applied magnetic field allow computation of the magnetization, which is linked to the mean orientation of the dipoles, as well as the birefringence. An anisotropic pair correlation function is also calculated, then transformed into a structure factor, in order to easily compare to experiments. Note that the suspensions considered here remain monophasic under a magnetic field. This is experimentally checked for all the samples and is also observed in simulations.

Let us begin with the orientation of the nanoparticles. If the ferrofluid is so dilute that the magnetic interparticle interaction is negligible, the magnetization M versus H follows the first Langevin's law ($M = M_{\text{sat}} \mathcal{L}_1(\xi) = M_{\text{sat}}(1/\coth(\xi) - 1/\xi)$, M_{sat} is the saturation value, $\xi = \mu_0 \mu H/kT$ is the ratio of the magnetic energy to the thermal energy), whereas the birefringence versus H follows the second Langevin's law ($\mathcal{L}_2 = 1 - 3\mathcal{L}_1/\xi^2$) [2]. If these magnetic interactions are no longer negligible, the magnetization M can be written in a mean field model: $M = M_{\text{sat}} \mathcal{L}_1(\xi_{\text{eff}})$ with $\xi_{\text{eff}} = \xi + \lambda \gamma \mathcal{L}_1(\xi_{\text{eff}})$, where λ is the effective field constant [10]. The simulations results perfectly follow the ideal laws for dilute ferrofluids; however, this is no longer true for concentrated ferrofluids as shown in figure 2, left. In the latter case, the mean field model allows adjusting the simulated curves, the best result being obtained with $\lambda = 0.22$, as already seen experimentally [19–21], and not with the usual value $\lambda = 0.33$ [22].

How is the structure modified, when the particles are orientated, and is there formation of chains? Examples of 2D structure factors under field are plotted in figure 3. On the left, the

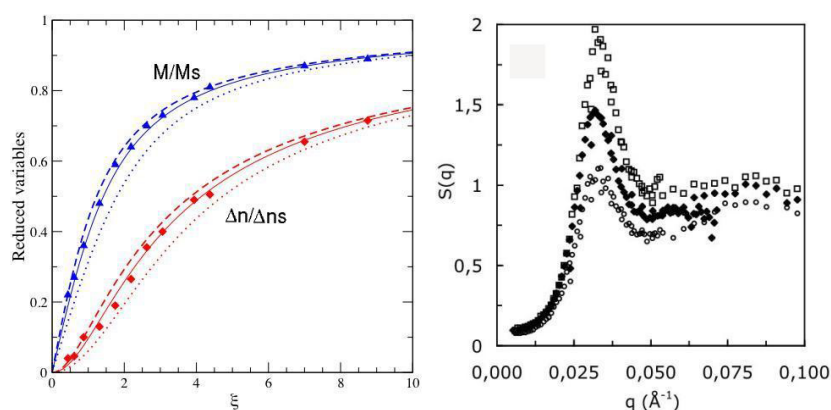


Figure 2. Left: reduced magnetization (triangles) and birefringence (diamonds) calculated for the ferrofluid studied here with $\phi = 10\%$. The dotted lines are ideal Langevin's laws. The dashed lines are calculated with the mean field model and $\lambda = 0.33$ while the full line is calculated with $\lambda = 0.22$. Right: structure factor without field (full diamond), q parallel to the magnetic field H (O) and q perpendicular to H (\square) for the ferrofluid with $\phi = 10.3\%$, a citrate concentration of 0.003 mol l^{-1} , and $H = 8200 \text{ Oe} = 656 \text{ kA m}^{-1}$. Measurements are performed on D22, ILL, Grenoble, France.

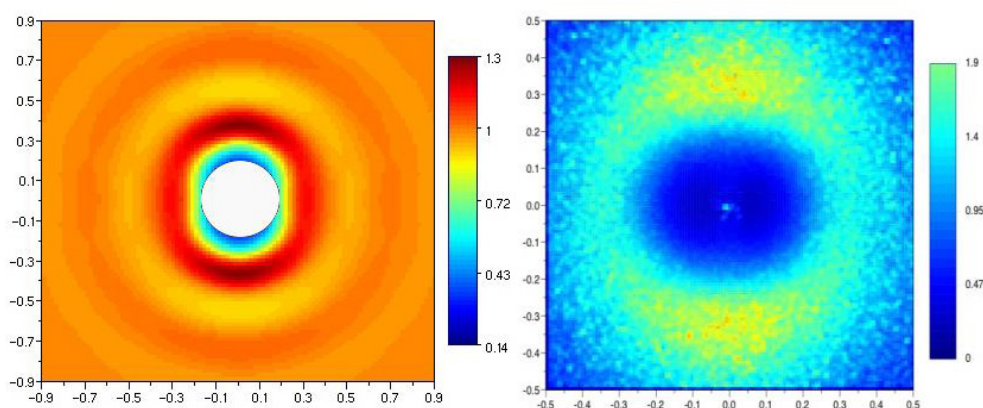


Figure 3. 2D structure factor calculated (left) or determined from the 2D experimental scattered intensity (right) under an applied magnetic field parallel to the horizontal direction. Simulation, $\phi = 0.10$ and $H = 1600 \text{ kA m}^{-1}$; experiment, $\phi = 0.097$ and $H = 656 \text{ kA m}^{-1}$. The axis indicates the q -values in nm^{-1} . The white disc on the left chart masks the unreliable q -range.

calculated $S(q)$ is anisotropic in the q -range plotted. The white disc in the centre masks the region of low wavevectors q (typically $q < 0.02 \text{ \AA}^{-1}$), where the results are no longer reliable because of the influence of the boundaries of the simulation box. On the right, the experimental $S(q)$ is also anisotropic in the q range plotted. Note that, at low q ($q < 0.02 \text{ \AA}^{-1}$, range not accessible by simulation), the data show an anisotropy of the compressibility (not shown here), which has been explained previously [20, 21]. From these 2D charts, $S(q)$ parallel and perpendicular to the field can be determined. An example is plotted in figure 2 (right) for the experimental $S(q)$ of figure 3 (right). It is compared to $S(q)$ without H . The peak is sharper in the direction perpendicular to the field and smoother in the direction parallel to the field. This means that the solution is better structured perpendicular to the field than parallel to it. This

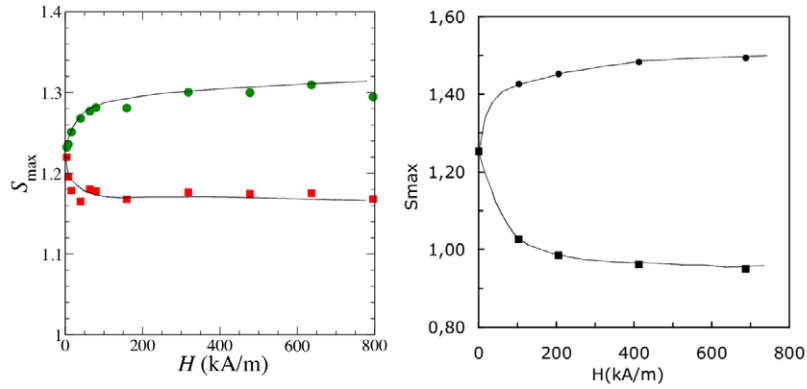


Figure 4. Value S_{\max} of the structure factor at the maximum of the peak as a function of the magnetic field, for the modelled system (left) and for the experimental system (right). Simulation, $\phi = 0.10$; experiment, $\phi = 0.097$. Squares, q parallel to the field; circles, q perpendicular to the field. The lines are guides for the eye.

is observed both for the calculated and the measured $S(q)$, as can be seen directly in figure 3, or in figure 4. However, the amplitude of the variation is larger in the experiment than in the calculation, which may result from the polydispersity of the nanoparticles in the real system.

Moreover, both the experimental and calculated structure factors, as well as the snapshots of the simulation box, show no evidence of chain formation [13]. These observations can be explained by the value of $\gamma/\phi = 34$ in the ferrofluid considered here: it is sufficiently high to induce an anisotropic structure under field but too small to enable the formation of chains. These results are moreover in good agreement with the recent simulations of Wang [23] as well as with the experiments of Butter [24] and Wagner [25].

4. Dynamics of the system: role of the dipolar interaction and of a magnetic field

4.1. Rotational dynamics

Without magnetic field, the characteristic time of the rotational diffusion of the nanoparticles τ_{rot} cannot be measured using the depolarized dynamic light scattering because of the huge absorption of maghemite. However, τ_{rot} can be computed from the autocorrelation function of the orientations [17]. In the range of volume fractions $1\% < \phi < 19\%$, the calculated τ_{rot} equals the Debye's law $\tau_{\text{rot}} = 1/(2D_o^r)$, and no noticeable influence of the hydrodynamic interactions is observed. The influence of the magnetic dipolar anisotropic interaction on the rotation dynamics is thus negligible. This probably results from the fact that the relevant parameter is not the dipolar parameter $\gamma/\phi = 34$ but an effective dipolar parameter which takes into account the fact that the particles can never come into contact because of the strong interparticle repulsion.

However, a time τ characteristic of the rotational properties of the nanoparticles can be measured and calculated. Indeed, experimentally, the system can be perturbed by applying a small magnetic field (35 or 70 Oe, 2.8 or 5.6 kA m⁻¹), which induces a birefringence in the dispersion, therefore a transmitted intensity between crossed polarizers [18, 26]. When the field is suppressed, the orientation of the nanoparticles relaxes towards random orientation and the measurement of the decay of the transmitted light allows determining a time τ . This experiment can be reproduced by non-equilibrium Brownian dynamics simulations. A first

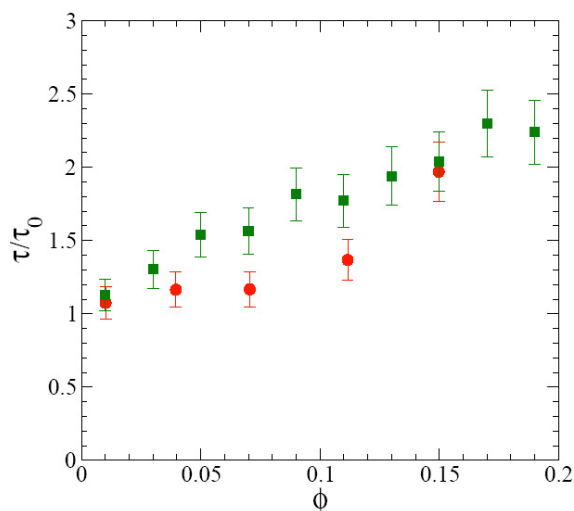


Figure 5. Comparison of experimental measurements (circles) and simulations (squares) of the relaxation of the induced birefringence under magnetic field: characteristic time τ of the rotation measured after a perturbation, normalized by the time τ_0 extrapolated at $\phi = 0$, as a function of ϕ . For the simulation, $\tau_0 = \tau_{\text{rot}}$.

stationary simulation is performed under magnetic field $H = 100$ Oe, then the field is set to zero and the evolution of the birefringence versus time is recorded. The procedure is repeated 40 times and the results are averaged in order to obtain a reasonable signal to noise ratio [17].

The experimental results are compared to the calculated times in figure 5 for volume fractions up to 20%: the time τ increases with ϕ in both experiments and simulations. These calculated τ are different from the τ_{rot} calculated without field except for low volume fractions, where they coincide (see figure 5). In the present case, the magnetic field is too high and the perturbation is too large to lie in the linear response domain.

Nevertheless, simulations and experiments are in qualitative agreement, the differences resulting from the simplifications of the model system compared with the experimental one. Firstly, contrary to the calculated relaxations, the experimental relaxation is not a pure exponential due to the size polydispersity of real nanoparticles: the relaxations can be modelled by the sum of an exponential and of a stretched exponential of larger characteristic time. In figure 5, the experimental value of τ corresponds to the pure exponential part of the experimental relaxation and may not be directly comparable to simulations. Secondly, in the simulations, the dipole is assumed to be fixed to the crystal axis (rigid dipole) whereas the dipole is softly linked to the crystal axis in maghemite for our range of sizes (the anisotropy energy is around 3–5 $k_B T$). This can reduce the influence of the dipolar interaction on the rotational relaxation time in the real system.

The increase of τ with ϕ observed in the response function to a pulse of magnetic field, but not in the correlation function in zero field, is likely to result from the collective orientation of the dipole moments. This can be studied by numerical simulations, which are of great benefit because they allow separating the influence of the different parameters, which is seldom achievable experimentally. For example, hydrodynamic interactions can be taken into account or not. It is shown that they have a weak but systematic influence on the rotational dynamics as they increase the relaxation time [17]. The weakness of this effect probably results from the dominating electrostatic repulsion in the interparticle potential. The simulations also allow

switching off the dipole moment, all the other parameters being kept constant. In this case, the time τ is constant with ϕ , which shows that this increase of τ with ϕ is indeed mainly due to the collective orientation of the dipole moments. Finally, the study of the rotation while freezing the translation shows no difference from the previous results, meaning that there is no detectable influence of the relaxation of the positions on the rotation of the nanoparticles.

In the same systems, for higher volume fractions ($\phi > 20\%$), the experiments show that the time τ drastically increases: the particles become blocked, and a glass forms [27]. In this area, the simulations can no longer be used due to the increasing timescales and to the difficulty of evaluating properly hydrodynamic interactions for concentrated systems. However, it is worth studying the dynamical arrest in a colloidal system, especially the rotation, far from being understood yet, as well as the coupling of rotation and translation. Also, ageing phenomena are observed in these concentrated systems [28]. All these points are currently under study.

4.2. Translational dynamics

In contrast to the case of rotational dynamics, the spatial scale has to be taken into account to investigate the translational dynamics. Moreover, one has to distinguish between individual and collective properties. Here, translation diffusion coefficients have been calculated and measured without magnetic field, which constitutes a reference in order to study the influence of the field on the translational movements of the particles.

The simulations allow us to obtain the translation diffusion coefficient of the nanoparticles on the local scale, using the calculation of the scattering intermediate functions $\mathcal{F}(\mathbf{q}, t)$. In the diffusive regime, $\mathcal{F}(\mathbf{q}, t) = \mathcal{F}(\mathbf{q}, 0) \exp(-Dq^2t)$ with D the diffusion coefficient, and it allows us to derive an effective diffusion coefficient $D_{\text{eff}}(q)$. The incoherent part gives the individual dynamics as a function of the spatial scale:

$$\mathcal{F}_{\text{inc}}(\mathbf{q}, t) = \frac{1}{N_p} \sum_{i=1}^{N_p} \langle e^{-i\mathbf{q}\cdot\mathbf{R}_i(0)} e^{i\mathbf{q}\cdot\mathbf{R}_i(t)} \rangle. \quad (3)$$

The coherent part gives a dynamics, the meaning of which depends on the spatial scale:

$$\mathcal{F}_{\text{coh}}(\mathbf{q}, t) = \frac{1}{N_p^2} \sum_{i,j=1}^{N_p} \langle e^{-i\mathbf{q}\cdot\mathbf{R}_i(0)} e^{i\mathbf{q}\cdot\mathbf{R}_j(t)} \rangle. \quad (4)$$

These two calculations with an applied magnetic field allow the determination of the diffusion coefficients in the directions parallel and perpendicular to the field. Quasi-elastic neutron scattering, here the neutron spin echo technique (NSE), yields $\mathcal{F}(\mathbf{q}, t)$. In the present work, the scattering is coherent so only $\mathcal{F}_{\text{coh}}(\mathbf{q}, t)$ has been determined experimentally, both without and with a magnetic field, using a special configuration of the set-up [29]. Note that the values of $D_{\text{eff}}(q)$ obtained from measurements and simulations cannot be directly compared because of the size polydispersity of the nanoparticles. Only the relative variations of D , D/D_0 , as a function of the different parameters can be compared, D_0 being the value of D at infinite dilution.

A set of the three quantities $D_{\text{inc}}^{\text{calc}}(q)$, $D_{\text{coh}}^{\text{calc}}(q)$, and $D^{\text{exp}}(q)$ obtained without field at $\phi = 0.1$ is plotted in figure 6(a). At large q , $D_{\text{inc}}^{\text{calc}}(q)$ and $D_{\text{coh}}^{\text{calc}}(q)$ tend towards the same value, which is a self-diffusion coefficient. The calculated D are close to the experimental determination. If $\phi \rightarrow 0$, all the values of $D(q \rightarrow \infty)$ tend towards D_0 , which is the limit of both the collective and the individual diffusion coefficients when interparticle interactions are negligible. Experimentally, D_0 can be measured in the dilute regime (here $\phi = 0.0001$) using dynamic light scattering or it can be extrapolated from the collective diffusion coefficient obtained by measuring the relaxation of the inhomogeneities of concentrations (by forced

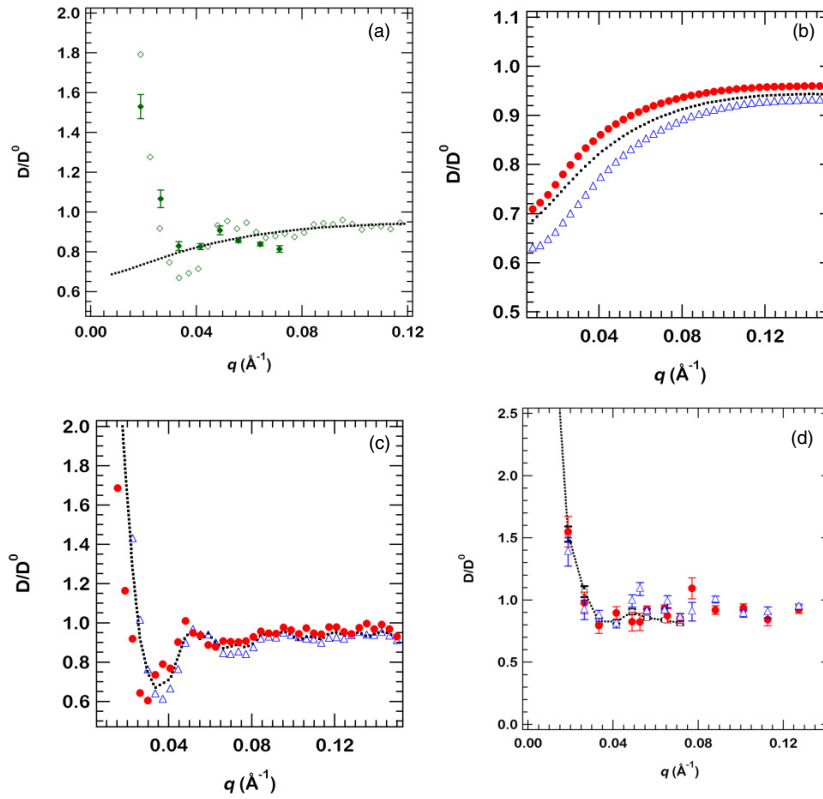


Figure 6. (a) Effective diffusion coefficient without field: coherent (open diamonds) and incoherent (dotted line) calculated and experimental determinations (full diamonds), $\phi = 0.1$; (b) calculated effective diffusion coefficients D_{eff} normalized by D_0 at infinite dilution with $H = 0$ (dotted line), q parallel to H (circles) and q perpendicular to H (triangles), $H = 790 \text{ kA m}^{-1}$, $\phi = 0.1$, incoherent part; (c) calculated effective diffusion coefficients D_{eff} normalized by D_0 at infinite dilution calculated with $H = 0$ (dotted line), q parallel to H (circles) and q perpendicular to H (triangles), $H = 790 \text{ kA m}^{-1}$, $\phi = 0.1$, coherent part; (d) effective diffusion coefficients D_{eff} measured by neutron spin echo, normalized by D_0 at infinite dilution, with $H = 0$ (dotted line), q parallel to H (circles) and q perpendicular to H (triangles). $H = 135 \text{ kA m}^{-1}$, $\phi = 0.1$, IN15, ILL, Grenoble, France.

Rayleigh scattering (FRS)) [30]. In the present study, $D_0^{\text{exp}} = 2 \times 10^{-11} \text{ m}^2 \text{ s}^{-1}$. *In the middle of the q range*, the coherent part oscillates, reproducing the oscillations of the structure factor, a phenomenon usually called de Gennes narrowing [31]. Experimentally, the shape of $D_{\text{eff}}^{\text{exp}}$ versus q is expected to be similar to the calculated coherent part; however, the oscillations are not observed, probably because of the polydispersity. *At low q* , the incoherent part, which corresponds to self-diffusion, shows that the self-diffusion is slowed down when the particle moves large distances (when $q \rightarrow 0$). However, the coherent part as well as the experiment show that the collective diffusion is accelerated when q tends towards zero. This latter effect results from the repulsive interactions between particles [32]. The extrapolation of the coherent part at $q = 0$ should lead to the macroscopic diffusion coefficient measured by FRS, which is for example $8 \times 10^{-11} \text{ m}^2 \text{ s}^{-1}$ for the sample with $\phi = 0.1$ corresponding to figure 6(a). This value is compatible with the values of $D_{\text{eff}}^{\text{exp}}$ at low q measured by NSE, even if an extrapolation of the NSE data is impossible because of the limited accessible q

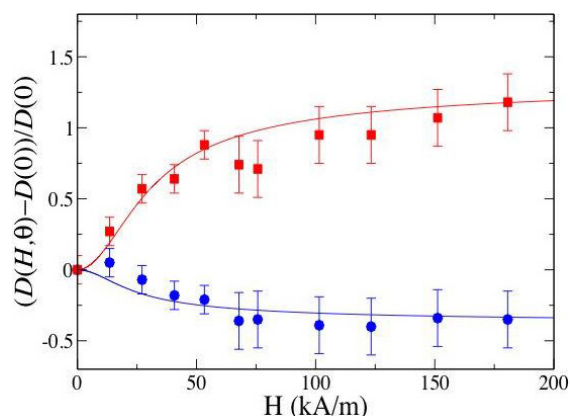


Figure 7. Reduced collective diffusion coefficient measured by FRS with an increasing applied magnetic field for $\phi = 0.05$ and $(\text{citrate}) = 0.08 \text{ mol l}^{-1}$. θ is the angle between the direction of the diffusion and the direction of the magnetic field. Squares: direction parallel to the field ($\theta = 0$). Circles: direction perpendicular to the field ($\theta = \pi/2$). The lines correspond to the model of [19] (no fitting parameter).

range, and because of the large correlation time, which becomes larger than the accessible times.

When a field is applied, a strong anisotropy of the structure factor is observed as well as a strong anisotropy of the macroscopic collective diffusion coefficient. Therefore, we expect an anisotropy of $D_{\text{eff}}(q)$. Indeed, the simulations show that the dynamics becomes anisotropic for all q values (figures 6(b) and (c)). However, this anisotropy remains small, and decreases when q increases. In contrast, within our experimental accuracy, no anisotropy is observed in the NSE experiments, whatever the volume fraction (ϕ from 0.1 to 0.16) and the citrate concentration (0.003 or 0.03 mol l^{-1}). As the calculated anisotropy is low, the experimental one may be even lower because of the polydispersity of the diameters of the nanoparticles and thus may not be detectable with this technique. At small q , $D_{\text{eff}}^{\text{exp}}$ should tend towards the values measured by FRS under field; however, this cannot be precisely checked because reliable data cannot be obtained for $q < 0.02 \text{ \AA}^{-1}$ as mentioned previously. For the sample studied here, the values obtained from FRS are indeed strongly anisotropic under field (see figure 7), as this has been observed in [19] for another ferrofluid. Moreover, this measured anisotropy is well described by the model developed in [19], which also allows explanation of the anisotropy of the structure factor at low q , thus of the compressibility [20].

This strong anisotropy observed in both the structure and the dynamics at low q is at contrast with the observations in the middle q range, i.e. on the scale of the interparticle distance, which corresponds to the q range probed with NSE and simulations. On this middle q scale, the structure is anisotropic: it is better structured in the direction perpendicular to the field. Note that this is associated at low q with a higher compressibility. At the same time, the translational diffusion is weakly anisotropic on this intermediate scale, whereas it is strongly anisotropic at low q . This difference of behaviour on the local scale compared with the behaviour on the macroscopic scale proves the strong influence of collective phenomena associated with the dipolar interaction.

This weak influence of the field on the translational diffusion at a local scale is moreover in good agreement with recent numerical simulations [33], which show that, in our conditions of dipolar interactions (quantified by the value of γ/ϕ), the anisotropy of the diffusion coefficient is around 10%.

5. Conclusion

In order to improve the understanding of ferrofluids, experimental measurements have been associated with simulations on a well defined magnetic fluid, with $\gamma/\phi = 34$. In the aqueous ferrofluids considered here, constituted of nanoparticles of diameters around 10 nm, with tunable electrostatic repulsion between the nanoparticles, the influence of the magnetic dipolar interaction is weak in zero field. In particular, they are dispersions of individual nanoparticles, i.e. no chains are formed. The rotational diffusion without field is similar to the rotation in a system without dipoles.

In a magnetic field, the experiments and the calculations show that no chains are formed in the present case. The rotation of the nanoparticles is strongly modified if the nanoparticles have been weakly orientated before determining the rotational diffusion, due to dominating collective effects. Moreover, the behaviour strongly depends on the spatial scale: at large scale (low q), the collective effects dominate: strong anisotropy of the structure and of the translational dynamics are observed. However, on the scale of the interparticle distance, the structure is anisotropic (simulations and experiments are in good agreement), but the translational diffusion calculated is weakly anisotropic. This could not be observed experimentally using the technique of neutron spin echo, probably because of the polydispersity of the nanoparticles and because of the value of the dipolar parameter, which is too low. In the future, the key point will be to prepare dispersions with high dipolar interactions and colloidal stability.

Acknowledgment

We acknowledge Delphine Talbot for the synthesis of the nanoparticles studied here.

References

- [1] Rosensweig R 1985 *Ferrohydrodynamics* (Cambridge: Cambridge University Press)
- [2] Berkowski B (ed) 1996 *Magnetic Fluids and Application Handbook* (Begell House: UNESCO)
- [3] Odenbach S (ed) 2003 *Magnetically Controllable Fluids and Their Applications* (Berlin: Springer)
- [4] Holm C and Weis J J 2005 The structure of ferrofluids: a status report *Curr. Opin. Colloid Interface Sci.* **10** 133–40
- [5] Klapp S H L 2005 Dipolar fluids under external perturbations *J. Phys.: Condens. Matter* **17** R525–50
- [6] Massart R 1980 Préparation de ferrofluides aqueux en l'absence de surfactant; comportement en fonction du pH et de la nature des ions présents en solution *C. R. Acad. Sci. Paris* **291** 1–2
- [7] Dubois E, Cabuil V, Boué F and Perzynski R 1999 Structural analogy between aqueous and oily magnetic fluids *J. Chem. Phys.* **111** 7147–60
- [8] Massart R, Dubois E, Cabuil V and Hasmonay E 1995 Preparation of monodisperse magnetic fluids *J. Magn. Mater.* **149** 1–5
- [9] Gazeau F, Boué F, Dubois E and Perzynski R 2003 Static and quasi-elastic neutron scattering on biocompatible ionic ferrofluids: magnetic and hydrodynamic interactions *J. Phys.: Condens. Matter* **15** S1305–34
- [10] Blums E, Cebers A and Maiorov M M 1997 *Magnetic Fluids* (Berlin: Walter Gruyter)
- [11] Parsegian V A, Fuller N and Rand R P 1979 *Proc. Natl Acad. Sci. USA* **76** 2750
- [12] Cousin F, Dubois E and Cabuil V 2003 Tuning the interactions of a magnetic colloidal suspension *Phys. Rev. E* **68** 021405
- [13] Mériguet G, Jardat M and Turq P 2004 Structural properties of charge-stabilized ferrofluids under a magnetic field: a brownian dynamics study *J. Chem. Phys.* **121** 6078–85
- [14] Mayer P and van Saarloos W 1982 *Physica A* **115** 21
- [15] Dickinson E, Allison S A and McCammon J A 1985 *J. Chem. Soc., Faraday Trans. 2* **81** 591
- [16] Jones R B and Alavi F N 1992 *Physica A* **187** 436
- [17] Mériguet G, Jardat M and Turq P 2005 Brownian dynamics investigation of magnetization and birefringence relaxations in ferrofluids *J. Chem. Phys.* **123** 144915

- [18] Hasmonay E, Dubois E, Bacri J C, Perzynski R, Stepanov V I and Raikher Yu L 1998 Static magneto-optical birefringence of size-sorted γ -Fe₂O₃ nanoparticle *Eur. Phys. J. B* **5** 859–67
- [19] Bacri J C, Cebers A, Bourdon A, Demouchy G, Heegard B M, Kashevsky B and Perzynski R 1995 Transient grating in a ferrofluid under magnetic field: effect of magnetic interaction on the diffusion coefficient of translation *Phys. Rev. E* **52** 3936
- [20] Gazeau F, Dubois E, Bacri J C, Boué F, Cebers A and Perzynski R 2002 Anisotropy of the structure factor of magnetic fluids under a field probed by small angle neutron scattering *Phys. Rev. E* **65** 031403
- [21] Mériquet G, Cousin F, Dubois E, Boué F, Cebers A, Farago B and Perzynski R 2006 What tunes the structural anisotropy of magnetic fluids under a magnetic field? *J. Phys. Chem. B* **110** 4378–86
- [22] Kittel C 1995 *Introduction to Solid State Physics* 7th edn (New York: Wiley)
- [23] Huang J P, Wang Z and Holm C 2005 Computer simulations of the structure of colloidal ferrofluids *Phys. Rev. E* **71** 061203
- [24] Butter K, Bomans P H H, Frederik P M, Vroege G J and Philipse A P 2003 Direct observation of dipolar chains in iron ferrofluids by cryogenic electron microscopy *Nat. Mater.* **2** 88–91
- [25] Wagner J, Fischer B and Autenrieth T 2006 Field induced anisotropy of charged magnetic colloids: a rescaled mean spherical approximation study *J. Chem. Phys.* **124** 114901
- [26] Hasmonay E, Bee A, Bacri J C and Perzynski R 1999 pH effect on an ionic ferrofluid: evidence of a thixotropic magnetic phase *J. Phys. Chem. B* **103** 6421–8
- [27] Mériquet G, Dubois E, Dupuis V and Perzynski R 2006 Rotational arrest in a repulsive colloidal glass *J. Phys.: Condens. Matter* submitted
- [28] Robert A, Wandersman E, Dubois E, Dupuis V and Perzynski R 2006 Glassy dynamics and aging in a dense ferrofluid *Europhys. Lett.* at press
- [29] Mezei F 1980 *Neutron Spin Echo (Springer Lecture Notes in Physics vol 128)* (Berlin: Springer)
- [30] Mériquet G, Dubois E, Bourdon A, Demouchy G, Dupuis V and Perzynski R 2005 Forced Rayleigh scattering experiments in concentrated magnetic fluids: effect of interparticle interactions on the diffusion coefficient *J. Magn. Magn. Mater.* **289** 39–42
- [31] Hayter J, Janninck G, Brochard-Wyart F and de Gennes P G 1980 *J. Phys. Lett.* **41** L-451
- [32] Pusey P N 1991 Colloidal suspensions *Liquids, Crystallization and Glass Transition* (Amsterdam: North-Holland) pp 763–932
- [33] Ilg P and Kröger M 2005 Anisotropic self-diffusion in ferrofluids studied via brownian dynamics simulations *Phys. Rev. E* **72** 031504